ELSEVIER

Journal of Chromatography A, 772 (1997) 39–48

JOURNAL OF CHROMATOGRAPHY A

Exactly solvable Ogston model of gel electrophoresis III. Percolation and sieving through two-dimensional gels

Gary W. Slater*, Joanne R. Treurniet

Department of Physics, 150 Louis-Pasteur, University of Ottawa, Ottawa, Ontario K1N 6N5, Canada

Abstract

Using our recently developed lattice model of gel electrophoresis, we study the sieving of large particles in random two-dimensional gels. We observe that a particle cannot migrate when the gel concentration exceeds a critical value, called the percolation threshold. The relationship between the percolation concentration and the particle size is determined. Finally, we show that in principle one can design 'templated' sieving matrices for special purposes.

Keywords: Ogston model; Ferguson plot; Gel electrophoresis; Pore size; Fiber radius; Percolation; Sieving matrices

1. Introduction

The electrophoretic mobility of a particle of size R in a gel of concentration C is determined by its electric charge and the kinetic resistance (also called the retardation effect) of the gel to its drift motion. The Ogston-Morris-Rodbard-Chrambach Model (OMRCM) of gel electrophoresis [1–9] assumes that the mobility μ of a (rigid) particle is given by

$$\frac{\mu(R,C)}{\mu_0} = \frac{V_A(R,C)}{V} = f(R,C) \qquad (1)$$

where μ_0 is the so-called free-solution mobility (which can also be a function of R), and V_A is the volume available to the particle within a total gel volume V. The reduced mobility $\mu^*(R,C) \equiv \mu(R,C)/\mu_0$, is thus assumed to be equal to the fractional gel volume $f(R,C)$ available to the particle. This model is often used to analyze data related to the separation of various particles and molecules, including nucleic acids, by gel electrophoresis. As we discussed in the first part of this series [8] (which we will denote Part I), this model uses the fractional available volume $f(R,C)$ as the only parameter to characterize the sieving properties of the gel, regardless of its architecture. In this sense, it is a mean-field model and it cannot account for the subtle effects of the correlations between the positions of the gel fibers. Also, it does not permit the study of very dense systems (high concentrations or large migrating particles) where the concept of percolating pathways is clearly of foremost importance.

Using the Poisson distribution, Ogston [1] derived the probability that a rigid sphere of diameter R can be placed in a random array of long, randomly oriented fibres:

$$f(R,C) = e^{-K(R)C} \qquad (2)$$

where C is the gel concentration and $K(R)$ is retardation coefficient. This expression is generally used in conjunction with Eq. (1) to analyze data. Eq. (2) can also be used for random two-dimensional systems if Poisson statistics apply. From Eq. (1) and (2), we get

*Corresponding author.

PII S0021-9673(97)00118-0

$$\ln [\mu(R,C)] = \ln [\mu_0] - K(R)C \quad (3)$$

The Ferguson plot, ln μ vs. C, is then predicted to be linear, and the mean pore size can be estimated from the retardation coefficient $K(R)$ (the slope) if the size R is known [3–6,10].

In Part I [8], we described the basic elements of a new lattice model of Ogston sieving. This model can be used to study an important class of problems, the sieving of rigid, spherically symmetric particles (in fact, one can also study the sieving of rod-like particles using this model; this will be the subject of a forthcoming article) in arbitrary gel structures, in the limit of low field intensities. For such systems, we demonstrated that Eq. (1) comes from a mean-field approximation. Our exact solutions indicated that $f(R, C)$ is not generally sufficient to describe the sieving properties of a gel because it does not consider the existence of percolating pathways in the gel and it neglects the fiber–fiber correlations. We also showed that the curvature of the Ferguson plot is actually related to the degree of disorder present in the gel structure. In Part II [9], we studied sieving in simple periodic two-dimensional gels because these ideal gels provide well-defined pore and fiber sizes (something which cannot be done unambiguously with random gels). We showed that a generalized retardation coefficient K can be defined for such gels, and that one can indeed derive an estimate of the effective pore size a_K, and fiber radius r_K from experimental data. In this paper (Part III), we present a study of random two-dimensional gels. In this case, the concepts of mean pore size and effective fiber radius are not clear. Therefore, we focus our attention on two different problems. First, we examine the conditions under which a particle cannot move through a random gel. This phenomenon has been observed by Serwer et al. [11] and is related to the concept of percolation [12]. Beyond a certain percolation concentration $C^*(R)$, a particle of size R has a zero mobility even though its available volume $f(R, C)$ is still finite. The relation $C^*(R)$ is compared to the mean pore size obtained from a Ferguson plot approach in order to understand the type of information one can derive from mobility measurements. Second, we demonstrate that one can in principle design periodic gels, with large and non-trivial 'templated' unit cells, for special purposes.

The paper is organized as follows. In Section 2, we briefly describe our model and how we calculate the exact zero-field mobilities of large particles migrating through random gels (the reader should refer to Part I and Part II for more technical details about the mathematical aspects). Section 3 describes typical results for one gel concentration and several particle sizes, as well as for one particle size and several gel concentrations. The concept of percolation is then explained and the percolation concentration $C^*(R)$ is determined. In Section 4, we show that one can design gels leading to almost any desired mobility vs. molecular size relationship. Our conclusions are found in Section 5.

2. Our model

After we developed a Monte Carlo method [7] to study the electrophoretic motion of hypercubic particles on hypercubic lattices (for any dimension $d > 1$; $d = 1$ gives the trivial result $\mu = 0$ in the presence of obstacles), we demonstrated in Part I how the zero-field electrophoretic mobility of this particle can actually be calculated exactly if we use a finite-size lattice with periodic boundary conditions (the gel fibers are represented by forbidden lattice sites). In this section, we briefly summarize the biased random-walk model and the mathematical methods used to calculate the exact electrophoretic mobility of $R \times R$ particles (R is thus the 'diameter' of the particle) moving in a two-dimensional random gel made of 1×1 obstacles (Fig. 1a). Note that for simplicity, only 1×1 obstacles will be considered in this article.

In the unbiased lattice random-walk model, the mean time duration of a jump is given by the Brownian time $\tau_B = L^2/(2D_0)$, where L is the lattice parameter and D_0 is the free solution diffusion coefficient of the particle. In the presence of an electric field E pointing in the $+x$ direction, the walk becomes biased in the x-direction and the reduced time duration $\tau^*(\varepsilon)$ of a jump for a particle of charge Q is given by [8,9]:

$$\tau^* = \frac{\tau}{\tau_B} = \frac{\tanh(\varepsilon)}{\varepsilon} \approx 1 + O(\varepsilon^2) \quad (4)$$

if the jump is made in the $\pm x$ direction, and by $\tau^*=1$ for $\pm y$ jumps. Here, $\varepsilon=QLE/(2k_BT)$ is the scaled field intensity, k_B is Boltzmann's constant, and T is the temperature. Note that to the first order in ε, the jumping frequency $1/\tau^*$ is the same for the x- and y- directions. To first order ε, the probabilities for the next jump to be in the $\pm x$ or $\pm y$ directions are [8,9]:

$$p_{\pm x}=\frac{1}{4}\pm\frac{\varepsilon}{4}+O(\varepsilon^3), \quad p_{\pm y}=\frac{1}{4} \tag{5}$$

where we clearly see the bias favouring $+x$ jumps. At each time step, the particle moves to one of the $2d$ ($=4$ in two-dimensions) adjacent sites according to the probabilities given by Eq. (5). If the particle overlaps with an obstacle after the jump, the move is rejected and the particle returns to its previous position; nevertheless, the time step counts. This jump rejection process models the hard core interactions between the solute and the gel matrix. To simplify the notation, all times and lengths will be dimensionless in the rest of this article (i.e., times will be measured in units of τ_B and lengths in units of L, such that velocities will be measured in units of L/τ_B), and only the reduced mobility $\mu^*\equiv\mu/\mu_0$ will be of interest.

The exact velocity of a particle on a lattice of size $N\times N$ (with periodic boundary conditions) can be calculated as follows (it can also be estimated using Monte Carlo simulations). We must first calculate the steady-state probability of presence p_i of the particle on the vacant sites of the lattice using rate equations describing the dynamics of the particle jumps (the transient period that follows the application of the field is not studied). This reduces the problem to a system of coupled linear equations for the p_i's (one equation for each empty lattice site). Once the p_i's are known, we calculate the mean velocity v by mutiplying the p_i's by the local electrophoretic velocities v_i for each site [8,9]. Since we study the low-field limit $\varepsilon\to 0$, we do all our calculations to first order in ε (we drop all higher order terms). At the end of the calculation, we simply take the limit for $\varepsilon\to 0$ in order to obtain the zero-field reduced mobility $\mu^*(R, \varepsilon=0)$. It is important to note that the result of such a calculation is exact, i.e. the mobility is exact for the specific distribution of obstacles and system size N under study.

In the case of large $R\times R$ particles moving through a random gel made of 1×1 obstacles (the case studied in this article), we can simplify the problem by increasing the size of the obstacles to $R\times R$ and shrinking the size of the migrating particle to 1×1 (see Fig. 1b) [9]. The two problems are mathematically identical, but the latter is somewhat easier to handle. We wrote a Mathematica© program that creates a gel structure, determines the corresponding

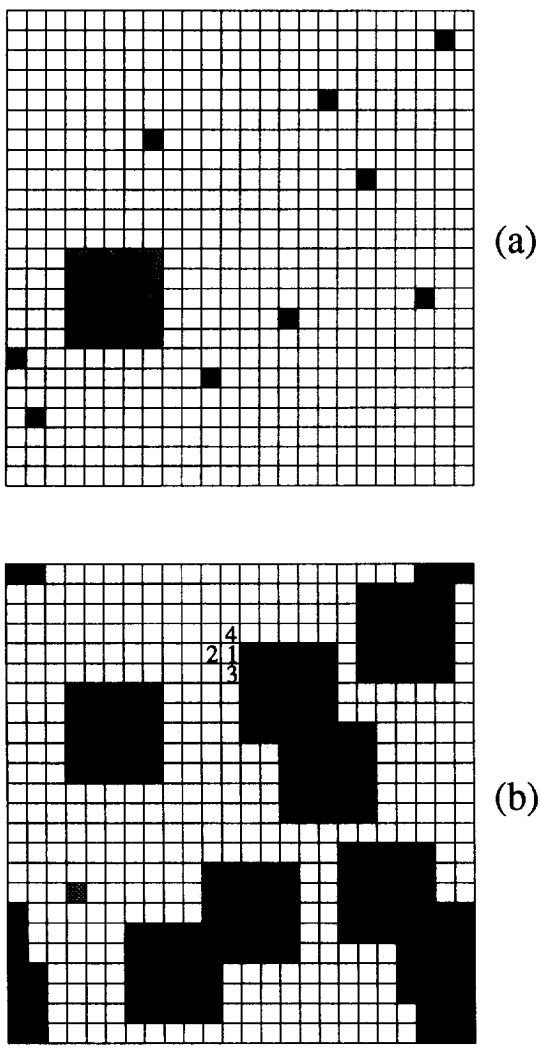

Fig. 1. (a) A random 2D gel of size $N=24$ and concentration $C=1/64$. The dark squares are 1×1 obstacles ('gel fibers') and the grey 5×5 square is the migrating particle. (b) A 1×1 particle is migrating in a gel made up of 5×5 obstacles. These two problems are mathematically equivalent.

rate equations, solves for the p_i's, and finally calculates the exact reduced mobility $\mu^*(R,C,\varepsilon \to 0)$.

As an example, we will show the exact results for the example given in Fig. 1. The 5×5 particle moving in the random gel structure of concentration $C=1/64$ shown in Fig. 1a and the 1×1 particle in Fig. 1b are equivalent. The position of 9 single-site obstacles (Fig. 1a) were chosen randomly with the constraint that they could not overlap. The size of the lattice is $N=24$, i.e. the system has 576 lattice sites with periodic boundary conditions. For simplicity, we will use Fig. 1b. The time-independent steady-state probability p_1 for the particle to occupy site $i=1$ (as shown in Fig. 1b) is due to the probability flow from the adjacent sites:

$$p_1 = \frac{1}{4}p_4 + \frac{1}{4}p_3 + \frac{1+\varepsilon}{4}p_2 + \frac{1+\varepsilon}{4}p_1 \qquad (6)$$

The first three terms on the r.h.s. of Eq. (6) simply calculate the total probability for a particle from one of the three empty adjacent sites (Nos. 4, 3 and 2, respectively) to jump onto site No. 1. The last term is due to the reflection of the particle on the obstacle. We thus have, $M=371$ such equations (one for each empty site on Fig. 1b), of which only 370 are independent. The normalization condition provides the 371st equation

$$\sum_{i=1}^{M} p_i = 1 \qquad (7)$$

Once the probabilities $P=\{p_1, p_2,...,p_M\}$ are calculated, we must calculate the local velocities $V=v_1,v_2,...,v_M$. For a biased random walk, the local velocity is simply given by $v_i = p_{+x}L_+ - p_{-x}L_-$; here, $L_\pm=1$ if there is no obstacle in the $\pm x$ direction, and 0 otherwise. The $p_{\pm x}$ are given by Eq. (5). Finally, the zero-field reduced electrophoretic mobility μ^* is related to the scalar product of the probability vector P with the velocity vector V as

$$\mu^* = \frac{1}{\mu_0}\lim_{\varepsilon\to 0}\frac{P\cdot V}{\varepsilon} \qquad (8)$$

where $\mu_0=1/2$ is the free solution (no obstacle) dimensionless mobility. For the example shown in Fig. 1, we get $\mu^*=0.348559...$ (with arbitrary precision). Again, this result is exact (no error bar).

If the gel structure is random, however, one must actually redo the calculation for a large number of systems (with different random patterns) of size $N\times N$ and average over the results. Fig. 2 shows the distribution of mobilities found for the $N=24$ lattice case studied above. One thousand systems were generated. The mean value is $\mu^*=0.5441\pm0.0042$, while the most probable value is around 0.6. We also note that 16 systems showed a zero mobility; in these cases, the obstacles created a vertical percolating wall across the system and the particle could not migrate over macroscopic distances. The distribution is quite wide (the standard-deviation is about 0.13), indicating that large concentration fluctuations can exist in such small systems. However, this wide distribution also suggests that one can build periodic gels, with e.g. a $N=24$ unit cell, with many different sieving properties. We will discuss this interesting point further in Section 4.

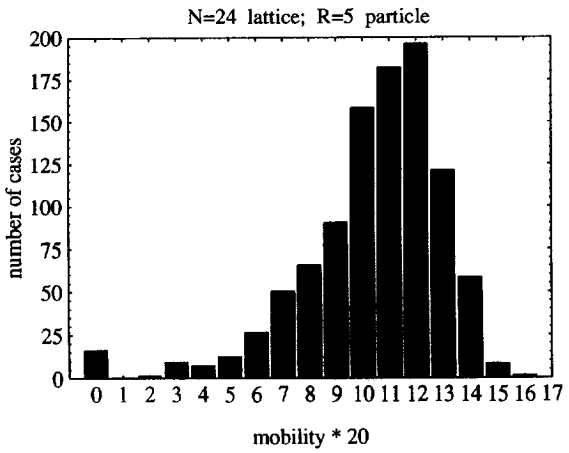

Fig. 2. Bar chart showing the number of times a mobility μ^* was obtained when one thousand $N=24$ and $C=1/64$ random lattice systems were generated. The migrating particle had a size $R=5$.

To find the true thermodynamic mobility, one must in principle find the exact reduced mobility μ^* for $N\to\infty$. In practice, one calculates the average mobility $\mu^*(R, N)$ for increasing values of N until an asymptotic value $\mu^*(R)$ is obtained. Note that the CPU time required to solve the $\approx N^2$ master equations increases roughly like N^6, while the standard-deviation decreases for larger values of N. Table 1 gives an example for the $C=1/64$ and $R=5$ system. The reduced mobility $\mu^*(R, N)$ essentially ceases to vary (to within the error bar) for system sizes $N\geq40$. The mobilities used for the rest of this article

Table 1
Reduced mobilities μ^* for a 5×5 particle moving in a gel of concentration $C=1/64$ for different lattice sizes N

Ensemble size (and number of non-percolating systems)	Lattice size N	Total number of obstacles	Average reduced mobility μ^* (with error bar)
Exact result (0)	8	1	0.661879...
1000 (6)	16	4	0.5814 (48)
1000 (16)	24	9	0.5441 (42)
200 (5)	32	16	0.5260 (83)
109 (4)	40	25	0.512 (12)
139 (3)	48	36	0.494 (17)
50 (4)	56	49	0.5187 (93)

The obstacles are of size 1×1. The average mobility is calculated using all the systems in the ensemble (see first column), including those which were not percolating (giving a zero-mobility). The error on the mobility is given in parenthesis, on the last one or two digits. As can be seen, the effect of the lattice size essentially disappears for systems sizes $N \geq 40$.

represent the asymptotic values obtained for $N=48$, unless specifically stated otherwise. The calculations were done on two IBM RISC/6000 workstations and required a minimum of 96 MB of RAM. The Mathematica programs are available upon request.

3. Percolation through a random gel

3.1. Mobility vs. particle size R

Table 2 gives the mobility μ^* vs. the particle size R for a gel of concentration $C=1/64$. The mobility essentially vanishes for $R>8$ because most systems are opaque to the molecule, i.e. the latter cannot find a percolating pathway through the random maze anymore. Similar calculations were performed for concentrations $C=1/256$, 2/256, 3/256, 5/256 and 6/256, and the same range of molecular sizes. Fig. 3 shows how the mobility varies with particle 'volume' R^2 for random gels of concentrations $C=4/256=1/64$ and 6/256.

Table 2
Reduced mobilities μ^* for particles moving in a gel of concentration $C=1/64$ and size $N=48$ for different particle sizes R

Ensemble size (and number of non-percolating systems)	Particle size R	Average reduced mobility μ^* (with error bar)
49 (48)	10	0.0034 (34)
56 (47)	9	0.040 (13)
65 (48)	8	0.057 (13)
200 (39)	7	0.149 (11)
200 (2)	6	0.335 (10)
139 (3)	5	0.494 (17)
59 (1)	4	0.666 (13)
110 (0)	3	0.8022 (56)
150 (1)	2	0.8943 (59)
58 (0)	1	0.9664 (2)

The obstacles are of size 1×1. The average mobility is calculated using all the systems in the ensemble (see first column), including those which were not percolating (giving a zero-mobility). The error on the mobility is given in parenthesis, on the last one or two digits.

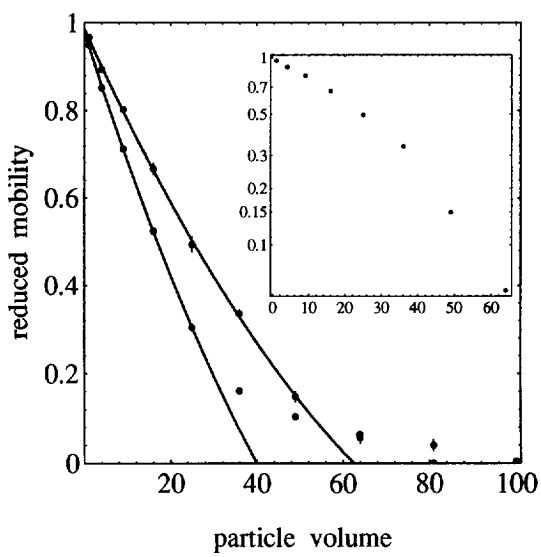

Fig. 3. Reduced mobility μ^* vs. particle 'volume' R^2 for 48×48 systems of concentrations $C=1/64$ (top line) and $C=6/256$ (bottom line). The solid lines show the best polynomial fits (see Eq. (9)); only the large mobility data was used for the fits. When the mobility is low, the data is affected by strong finite-size effects. Insert: A semi-log plot of the $C=1/64$ data.

Table 3
Parameters found when fitting the mobility μ^* vs. particle volume R^2 data using Eq. (9) for various gel concentrations C

C	$\mu^*(0, C)$	r_2	r_4	R^*
1/256	0.9932	14.6	22.1	16.7
2/256	0.9909	10.1	16.4	11.1
3/256	0.9882	8.03	12.0	9.36
4/256	0.9850	6.80	10.1	7.91
5/256	0.9824	6.19	9.93	6.78
6/256	0.9777	5.67	8.81	6.32

The insert of Fig. 3 shows a plot of $\ln[\mu^*]$ vs. R^2 for $C=1/64$. The OMRCM would predict a straight line for this plot. As we found in Part I and Part II, the exponential dependence predicted by the OMRCM is not found to give a good description, except, perhaps, close to zero molecular size. Of course, an exponential dependence cannot account for the existence of a percolation threshold. In order to study percolation, we must use a polynomial fit. Indeed, an excellent fit of the data is provided by a polynomial function of the form:

$$\mu^*(R, C) \approx \mu(0, C) - \left(\frac{R}{r_2(C)}\right)^2 + \left(\frac{R}{r_4(C)}\right)^4 \qquad (9)$$

The fits for $C=4/256$ and $6/256$ are shown in Fig. 3. Table 3 gives the fitting parameters $\mu(0,C)$, r_2 and r_4 vs. gel concentration C, as well as the critical molecular size R^* for which the fits predicts $\mu^*(C,R)=0$. For example, the fits in Fig. 3 give $R^*(C=4/256)=7.91$ and $R^*(C=6/256)=6.32$. Note that the points for the large particle volumes R^2, close to the percolating limit, cannot be explained by the fit; this is an effect of the limited size of the lattice (48×48), and is reduced when larger lattices are used. For example, the mobility of a $R=7$ particle was found to $\mu^*=0.104\pm0.007$ when 200 systems of size 48×48 and concentration $C=6/256$ were generated; a study done with larger 64×64 systems gave $\mu^*=0.02\pm0.02$ with 30 systems generated, in agreement with the fact that our fit predicts a critical size $R^*=6.32$ for this concentration. The fits must use only the points that are far from the percolation threshold otherwise strong finite-size effects affect the results. It is worth mentioning, however, that the $R=R^*$ particle does not have a zero fractional available volume $f(R^*,C)$: the mobility is negligible because there is no percolating pathway through the gel. Lack of migration in random gels has been reported by Serwer et al. [11].

If we use R^* to characterize the pores of this gel, our results (Table 3) would indicate that the 'pore size' (diameter) is given roughly by $\bar{a}=R^*\approx(0.67/C)^{0.54}$. The exponent 0.54 found here is slightly larger than the one we found (0.50) for periodic gels in Part II. Note also that the first coefficient of the fit appears to vary like $r_2\approx(0.59/C)^{0.53}$, showing again an exponent slightly larger than 1/2.

3.2. Mobility vs. gel concentration C

Table 4 gives the mobility $\mu^*(R=5, C)$ of a 5×5 particle for various gel concentrations. Here, the mobility essentially vanishes for concentrations exceeding approximately 8/256 because of the absence

Table 4
Reduced mobilities μ^* for $R=5$ particles moving in a gel of size $N=48$ for different gel concentrations C

Ensemble size (and number of non-percolating systems)	Gel concentration C	Average reduced mobility μ^* (with error bar)
39 (0)	1/256=0.390625%	0.8742 (37)
57 (0)	2/256=0.78125%	0.7618 (51)
57 (0)	3/256=1.171875%	0.624 (13)
139 (3)	4/256=1.5625%	0.494 (17)
45 (4)	5/256=1.953125%	0.387 (22)
75 (18)	6/256=2.34375%	0.247 (18)
48 (21)	8/256=3.125%	0.095 (15)
53 (50)	10/256=3.90625%	0.0103 (65)

The obstacles are of size 1×1. The average mobility is calculated using all the systems in the ensemble (see first column), including those which were not percolating (giving a zero-mobility). The error on the mobility is given in parenthesis, on the last one or two digits.

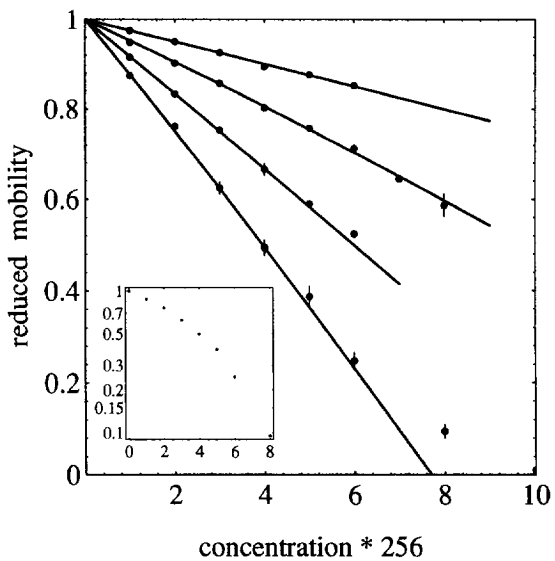

Fig. 4. Reduced mobility μ^* vs. gel concentration C for the particle sizes (from top to bottom) $R=1$, 2, 3, 4, 5 in a 48×48 gel. The solid lines show the best polynomial fits (see Eq. (10)). Insert: A semi-log plot of the $R=5$ data.

of percolating pathways for large concentrations. Fig. 4 shows the reduced mobility μ^* vs. gel concentration C for particles of size $R=2$, 3, 4, and 5 (the size $R=1$ was studied in Part I). The insert shows $\ln[\mu]$ vs. C for the 5×5 particle; according to the OMRCM, this plot should exhibit a straight line. As shown in Part II, a much better fit to data is provided by the polynomial:

$$\mu^*(R, C) \approx 1 - \left(\frac{C}{c_1(R)}\right) - \left(\frac{C}{c_2(R)}\right)^2 \qquad (10)$$

The fitting parameter $c_1(R)$ is the same for random and periodic systems since the mobility must be the same for all gel architectures in the zero-concentration limit. These coefficients were calculated with extremely high precision in Part II. Table 5 thus gives the fitting parameters c_1 and c_2 for $1\leq R\leq5$. The percolating concentration $C^*(R)$ for which Eq. (10) predicts a zero mobility is also given.

Again, in spite of the fact that a particle of size R can still be placed in the gel for concentrations $C>C^*$, it has a zero net mobility because it cannot find a percolating pathway through the gel. Beyond C^*, the particle cannot migrate over macroscopic

Table 5
Parameters found when fitting the mobility μ^* vs. gel concentration C data using Eq. (10) for various particle sizes R

Particle size R	c_1	c_2	C^*
1	0.467	1.06	104/256
2	0.158	0.680	38.4/256
3	0.0781	0.6114	19.7/256
4	0.0463	0.451	11.7/256
5	0.0306	0.240	7.71/256

Parameter c_1 was taken from Ref. [9]. For $R>5$, there were too many points affected by finite-size effects to obtain useful fits.

distances. If we now use $C^*(R)$ to characterize the sieving properties of the gel, we obtain, from Table 5, that $C^*\approx(0.66/R)^{1.70}$, which can be inverted to give $\bar{a}=R\approx(0.49/C)^{0.59}$. The exponent found here is slightly larger than the one found in the Section 3.1 (0.54). For a periodic gel, we found the relation $\bar{a}\approx(0.86/C)^{0.50}$ in Part II. The apparent mean pore size is therefore smaller in random gels for the same concentration, which is not surprising since the heterogeneity reduces the mobility (see Part I for a comparison). The fact that the exponent is somewhat larger remains to be explored in more detail but it may explain why an exponent of 0.50 is rarely found when the mean pore size of a gel is studied using the Ferguson plot.

Clearly, these two cases demonstrate that the concept of percolation is extremely important for random gels, especially for 'large' concentrations. In Parts I and II, we also showed that the correlation between the position of the obstacles was important to understand the low-concentration mobilities. Knowing this, one should be able, at least in principle, to design gel structures to achieve special separation goals. The easiest way to do this is to design a small gel structure that provides the required separation, and then to repeat it in order to form an infinite, periodic gel. This is the approach we take in the next section.

4. Designing gel structures

We saw in Fig. 2 that when a small system is used ($N=24$ in this case), large mobility fluctuations could be observed for the $R=5$ particle even though

all these gels had the same concentration. In a real gel, the structural effects fluctuate from region to region, which certainly lead to large mobility fluctuations during the migration. However, since the particle migrates over macroscopic distances, they all visit the same average gel and they acquire the same average long-time mobility (small residual differences between the migrating paths of individual particles may explain some of the band broadening).

Periodic sieving lattices can be built using the method described earlier by Volkmuth and Austin [13]. These lattices actually use a simple one obstacle unit cell that is repeated evenly in all directions. Here, we want to see if using a more complicated unit cell could lead to interesting sieving properties. For instance, Fig. 2 indicates that 24×24 unit cells could lead to any mobility in the range of 0.00 to 0.75, depending on the structure chosen. Can we build such a gel in order to optimize the separation in a specific size range?

Fig. 5 shows the mobilities of $R=1$, $R=2$, $R=3$, $R=4$ and $R=5$ particles in thirty different 16×16 random $C=1/32$ gels (with periodic boundary conditions). As we can see, certain gels have quite atypical sieving properties. While the mobility of the small 1×1 particle does not fluctuate much, the mobility of the largest ones is often zero because of the percolation problem discussed in Section 3. For gel No. 26, we note that the particles have very similar mobilities (the largest two even co-migrate), a remarkable result since they must have access to very different available fractional volumes. This result is normally typical of self-similar (fractal) gel structures (this will be the topic of a forthcoming article)! On the other hand, gel No. 28 shows even stranger results: the $R=4$ particle is actually slower than the $R=5$ one! Gel No. 5 provides reasonable mobilities for all particles as well as a good separation over the entire range. Fig. 6 shows these three different gel structures. Clearly, the narrow channels and funnel structures are responsible for the behaviour observed.

As we can see, simple cell structures like the ones possible for $C=1/32$ periodic cells of size 16×16, can lead to a very wide range of sieving properties. Instead of using randomly formed chemical gels, we therefore suggest to design two-dimensional gels, following the method proposed in Ref. [13], but with larger unit cells. This could provide high-selectivity separations for specific applications.

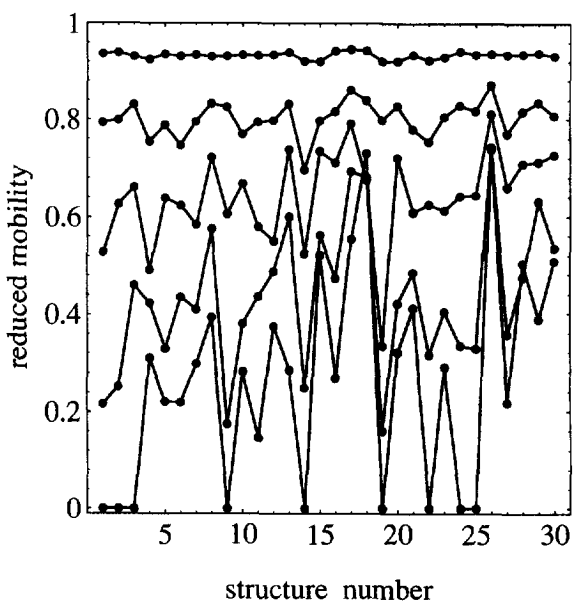

Fig. 5. Reduced mobility μ^* for five different particles in 30 different 16×16 random $C=1/32$ gels. The lines, from top to bottom, are for sizes $R=1$, $R=2$, $R=3$, $R=4$ and $R=5$.

5. Discussion

In this article, we have used our exactly solvable Ogston-like model of gel electrophoresis to study the percolating properties of random two-dimensional gels. This version of the model is valid in the zero-field limit and for simple hard-core interactions between the migrating particles and the gel fibers. Again, we find that the electrophoretic mobility is not in general proportional to the fractional available volume f, as assumed by all OMRCM-like models. Indeed, the existence of the percolation threshold concentration C^* cannot be explained by a mean-field model. For low concentrations, an exponential fit might appear to be satisfactory. However, a polynomial fit can do better over a larger range of concentrations; more importantly, however, such fits allow us to extrapolate to $C=C^*$. Fig. 3 shows that the mobility decreases nearly linearly with particle volume over a wide range of sizes.

We used the size of the largest particle that can

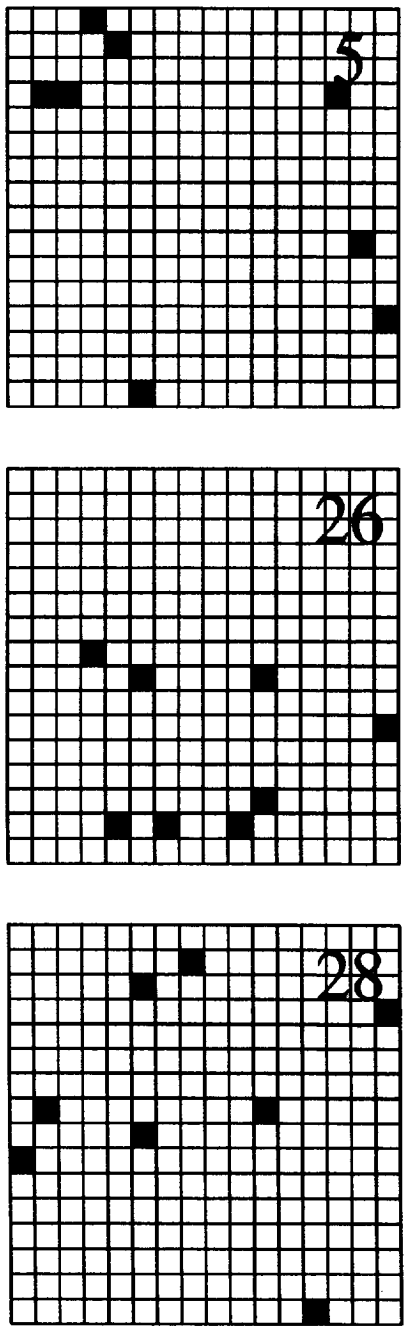

Fig. 6. Gel systems Nos. 5, 26 and 28 corresponding to the results obtained in Fig. 5.

move in a gel as a measure of the mean pore size, as suggested by Serwer and Hayes [11]. Our results demonstrate that for a given concentration, random gels provide more resistance to the motion. The relationship between the pore size and the gel concentration, written as $\bar{a} \sim C^{-y}$, suggests an exponent $y \approx 0.54$–0.59, slightly larger than for a periodic gel (0.50).

We have observed that the mobility fluctuates enormously for random systems that are built using small unit cells and periodic boundary conditions. This suggests that one can use such systems to custom-build sieving matrices for specific applications. One can design matrix structures that are very selective. Surprisingly, one can also build structures which lead to essentially molecular size independent mobilities over a wide range of sizes.

During the Prague meeting where these results were first presented, prof. S. Hjertén described preliminary data on 'templated' gels which showed that gels with certain specific structures can increase the separation of particles. More recently, Rill et al. [14] showed that nanostructured, 'templated' gels give different sieving results. This is essentially what Fig. 6 demonstrates. For example, gel No. 28 affects the $R=4$ particle more than the others because the two obstacles in the middle of the gel form a channel of width 4. Our theoretical approach can in principle be used to design templated systems. This is currently under investigation.

In conclusion, we have shown that percolation is an important factor to consider when large particles migrate in dense random gels. However, it is possible to design gel structures that possess almost arbitrary sieving properties if these percolating properties are used properly.

Acknowledgments

The authors would like to thank Hong Guo and Professor Hjertén for useful discussions. This work was supported by a Research Grant from the National Science and Engineering Research Council of Canada to GWS.

References

[1] A.G. Ogston, Trans. Farady Soc. 54 (1958) 1754–1757.

[2] C.J.O.R. Morris, in H. Peeters (Editor), Protides of the Biological Fluids, 14th Colloquium. Elsevier, New York, 1967, pp. 543–551.
[3] D. Rodbard, A. Chrambach, Proc. Nat. Acad. Sci. USA 65 (1970) 970–977.
[4] D. Tietz, in A. Chrambach, M.J. Dunn, B.J. Radola (Editors), Advances in Electrophoresis, Vol. 2, VCH, Weinheim, 1988, pp. 109-169.
[5] P. Serwer, Electrophoresis 4 (1983) 375–382.
[6] G.W. Slater, J. Rousseau, J. Noolandi, C. Turmel, M. Lalande, Biopolymers 27 (1988) 509–524.
[7] G.W. Slater, H.L. Guo, Electrophoresis 16 (1995) 11–15.
[8] G.W. Slater, H.L. Guo, Electrophoresis 17 (1996) 977–988.
[9] G.W. Slater, H.L. Guo, Electrophoresis 17 (1996) 1407–1415.
[10] K.A. Ferguson, Metabolism 13 (1964) 985–1002.
[11] P. Serwer, S.J. Hayes, Anal. Biochem. 158 (1986) 72–78.
[12] D. Stauffer, A. Aharony, Introduction to Percolation Theory, Taylor and Francis, London 1992.
[13] W.D. Volkmuth, R.H. Austin, Nature 358 (1992) 600–602.
[14] R.L. Rill, B.R. Locke, Y. Liu, J. Dharia, D. Van Winkle, Electrophoresis 17 (1996) 1304–1312.